LHC and γC Probes of the Scalar Sector of the Randall-Sundrum Model

Jack Gunion
Davis Institute for High Energy Physics, U.C. Davis

Presented by M. Velasco

RS Collaborators: M. Battaglia, S. de Curtix, A. De Roeck, D. Dominici, B. Grzadkowski, M. Toharia, J. Wells

γC Collaborators: D. Asner, J. Gronberg, M. Velasco

Cornell LC Workshop, 7/13/2003

Previous work:

- $\xi = 0$:

1. S. B. Bae, P. Ko, H. S. Lee and J. Lee, Phys. Lett. B 487, 299 (2000) [arXiv:hep-ph/0002224].
2. H. Davoudiasl, J. L. Hewett and T. G. Rizzo, Phys. Rev. Lett. 84, 2080 (2000) [arXiv:hep-ph/9909255].
3. K. Cheung, Phys. Rev. D 63, 056007 (2001) [arXiv:hep-ph/0009232].
4. H. Davoudiasl, J. L. Hewett and T. G. Rizzo, Phys. Rev. D 63, 075004 (2001) [arXiv:hep-ph/0006041].
5. S. C. Park, H. S. Song and J. Song, Phys. Rev. D 63, 077701 (2001) [arXiv:hep-ph/0009245].

- $\xi \neq 0$:

1. G. Giudice, R. Rattazzi, J. Wells, Nucl. Phys. B595 (2001), 250, hep-ph/0002178.
2. C. Csaki, M.L. Graesser, G.D. Kribs, Phys. Rev. D63 (2001), 065002-1, hep-th/0008151.
3. T. Han, G. D. Kribs and B. McElrath, Phys. Rev. D 64, 076003 (2001) [arXiv:hep-ph/0104074].

4. M. Chaichian, A. Datta, K. Huitu and Z. h. Yu, Phys. Lett. B 524, 161 (2002) [arXiv:hep-ph/0110035]. These authors (see their Appendix A) employ the same full mixing procedure as that employed in our paper (hep-ph/020619). Some of their results can be usefully compared to the LHC discussion of hep-ph/020619.
5. J. L. Hewett and T. G. Rizzo, hep-ph/0202155. As pointed out in their recent revision of this work dated July 2, 2003, our paper (hep-ph/0206192) appeared 4 months after their original hep-ph submission. However, their results at that time, in their previous presentations, and in all but the most recent presentations, were incorrect except at rather small ξ values due to the fact that they employed the small ξ approximations to the mixing/diagonalization procedures that were given in Giudice etal., hep-ph/0002178. The revision of July 2, 2003 comes some 12 months after our hep-ph/0206192 preprint. Their results now appear to be in accord with ours. Our work was, of course, performed completely independently of their work and was fully in progress at the time of their earliest presentation.
6. C. Csaki, M. Graesser, L. Randall and J. Terning, Phys. Rev. D 62, 045015 (2000) [arXiv:hep-ph/9911406].

Outline

- The parameter space
- Basics of the couplings
- LHC/γC Complementarity
- Conclusions

Presuming the new physics scale to be close to the TeV scale, there can be a rich new phenomenology in which Higgs and radion physics intermingle if the $\xi R \widehat{H}^\dagger \widehat{H}$ mixing term is present in $\mathcal{L}$.

References:

- D. Dominici, B. Grzadkowski, J. F. Gunion and M. Toharia, "The scalar sector of the Randall-Sundrum model," arXiv:hep-ph/0206192.
- M. Battaglia, S. De Curtis, A. De Roeck, D. Dominici and J. F. Gunion, "On the complementarity of Higgs and radion searches at LHC," arXiv:hep-ph/0304245.

- **D. M. Asner, J. B. Gronberg and J. F. Gunion, "Detecting and studying Higgs bosons in two-photon collisions at a linear collider," Phys. Rev. D 67, 035009 (2003) [arXiv:hep-ph/0110320].**

Randal-Sundrum Review

Some possibly very dramatic changes in phenomenology.

- There are two branes, separated in the 5th dimension (y) and $y \to -y$ symmetry is imposed. With appropriate boundary conditions, the 5D Einstein equations $\Rightarrow$

$$ds^2 = e^{-2\sigma(y)}\eta_{\mu\nu}dx^\mu dx^\nu - b_0^2 dy^2, \tag{1}$$

  where $\sigma(y) \sim m_0 b_0 |y|$.

- $e^{-2\sigma(y)}$ is the warp factor; scales at $y = 0$ of order M_{Pl} on the hidden brane are reduced to scales at $y = 1/2$ of order TeV on the visible brane.

- Fluctuations of $g_{\mu\nu}$ relative to $\eta_{\mu\nu}$ are the KK excitations $h^n_{\mu\nu}$.

- Fluctuations of $b(x)$ relative to b_0 define the radion field.

- In addition, we place a Higgs doublet $\widehat{H}$ on the visible brane. After various rescalings, the properly normalized quantum fluctuation field is called h_0.

Including the ξ mixing term

- We begin with

$$S_\xi = \xi \int d^4x \sqrt{g_{\rm vis}} R(g_{\rm vis}) \widehat{H}^\dagger \widehat{H} \,, \tag{2}$$

where $R(g_{\rm vis})$ is the Ricci scalar for the metric induced on the visible brane.

- A crucial parameter is the ratio

$$\gamma \equiv v_0/\Lambda_\phi \,. \tag{3}$$

where Λ_ϕ is vacuum expectation value of the radion field.

- After writing out the full quadratic structure of the Lagrangian, including $\xi \neq 0$ mixing, we obtain a form in which the h_0 and ϕ_0 fields for $\xi = 0$ are mixed and have complicated kinetic energy normalization.

  We must diagonalize the kinetic energy and rescale to get canonical

normalization.

$$h_0 = \left(\cos\theta - \frac{6\xi\gamma}{Z}\sin\theta\right) h + \left(\sin\theta + \frac{6\xi\gamma}{Z}\cos\theta\right)\phi$$

$$\equiv dh + c\phi \tag{4}$$

$$\phi_0 = -\cos\theta\frac{\phi}{Z} + \sin\theta\frac{h}{Z} \equiv a\phi + bh\,. \tag{5}$$

- In the above equations

$$Z^2 \equiv 1 + 6\xi\gamma^2(1 - 6\xi)\,. \tag{6}$$

$Z^2 > 0$ is required to avoid tachyonic situation.

This $\Rightarrow$ constraint on maximum neg. and pos. ξ values.

- The process of inversion is very critical to the phenomenology and somewhat delicate.

The result found is that the physical mass eigenstates h and ϕ cannot be too close to being degenerate in mass, depending on the precise values of ξ and γ; extreme degeneracy is allowed only for small ξ and/or γ.

Using this inversion, for given ξ, γ, m_h and m_ϕ we compute Z^2, $m_{h_0}^2$ and $m_{\phi_0}^2$, θ to obtain a, b, c, d in Eqs. (4) and (5).

- **Net result**

4 independent parameters to completely fix the mass diagonalization of the scalar sector when $\xi \neq 0$. These are:

$$\xi\,, \quad \gamma\,, \quad m_h\,, \quad m_\phi\,, \tag{7}$$

where we recall that $\gamma \equiv v_0/\Lambda_\phi$ with $v_0 = 246\ \mathrm{GeV}$.

The quantity $\widehat{\Lambda}_W = \frac{1}{\sqrt{3}}\Lambda_\phi$ fixes the KK-graviton couplings to the h and ϕ and

$$m_1 = x_1 \frac{m_0}{M_{Pl}} \frac{\Lambda_\phi}{\sqrt{6}} \tag{8}$$

is the mass of the first KK graviton excitation (x_1 is the first zero of the Bessel function J_1 ($x_1 \sim 3.8$)

m_0/M_{Pl} is related to the curvature of the brane and should be a relatively small number for consistency of the RS scenario.

- Sample parameters that are safe from precision EW data and RunI Tevatron constraints are $\Lambda_\phi = 5$ TeV ($\Rightarrow \widehat{\Lambda}_W \sim 3$ TeV) and $m_0/M_{Pl} = 0.1$.

  The latter $\Rightarrow m_1 \sim 780$ GeV; i.e. m_1 is typically too large for KK graviton excitations to be present, or if present, important, in h, ϕ decays.

  But, KK excitations in this mass range (and much higher) will be observed and well measured at the LHC.

- Given this choice, we complete the inversion by writing out the kinetic energy terms of the complete Lagrangian using the substitutions of Eqs. (4) and (5) and demanding that the coefficients of $-\frac{1}{2}h^2$ and $-\frac{1}{2}\phi^2$ agree with the given input values for m_h^2 and m_ϕ^2.

  Results shown take $m_0/M_{Pl} = 0.1$.

- KK excitation probably observable at LHC

  Will provide important information.

1. **Mass gives m_1 in above notation.**
2. **Excitation spectrum as a function of m_{jj} determines m_0/M_{Pl}.**
3. **Combine ala Eq. (8) to get Λ_ϕ.**
   This will really help in LHC-only study of Higgs sector.

The Couplings

The $f\overline{f}$ and VV couplings

- **The VV couplings**
  - The h_0 has standard ZZ coupling.
  - The ϕ_0 has ZZ coupling deriving from the interaction $-\frac{\phi_0}{\Lambda_\phi}T^\mu_\mu$ using the covariant derivative portions of $T^\mu_\mu(h_0)$.

  The result for the $\eta_{\mu\nu}$ portion of the ZZ couplings is:

$$g_{ZZh} = \frac{g\, m_Z}{c_W}(d+\gamma b)\ , \quad g_{ZZ\phi} = \frac{g\, m_Z}{c_W}(c+\gamma a)\ . \tag{9}$$

  g and c_W denote the $SU(2)$ gauge coupling and $\cos\theta_W$, respectively. The WW couplings are obtained by replacing gm_Z/c_W by gm_W.

- **The $f\overline{f}$ couplings**
  - The h_0 has standard fermionic couplings.

- The fermionic couplings of the ϕ_0 derive from $-\frac{\phi_0}{\Lambda_\phi}T^\mu_\mu$ using the Yukawa interaction contributions to T^μ_μ.
- One obtains results in close analogy to the VV couplings just considered:

$$g_{f\bar{f}h} = -\frac{g\,m_f}{2\,m_W}(d+\gamma b)\,, \quad g_{f\bar{f}\phi} = -\frac{g\,m_f}{2\,m_W}(c+\gamma a)\,. \tag{10}$$

- Note same factors for WW and $f\bar{f}$ couplings.

The gg and $\gamma\gamma$ couplings

- There are the standard loop contributions, except rescaled by $f\bar{f}/VV$ strength factors g_{fVh} or $g_{fV\phi}$.

- In addition, there are anomalous contributions, which are expressed in terms of the SU(3)×SU(2)×U(1) β function coefficients $b_3 = 7$, $b_2 = 19/6$ and $b_Y = -41/6$.

- The anomalous couplings of h and ϕ enter only through their radion admixtures, $g_h = \gamma b$ for the h, and $g_\phi = \gamma a$ for the ϕ.

Couplings

- First, consider the $f\overline{f}/VV$ couplings of h and ϕ relative to SM, taking $m_h = 120$ GeV and $\Lambda_\phi = 5$ TeV.

  For the chosen value of $m_0/M_{Pl} = 0.1$, once m_h and Λ_ϕ are fixed, the remaining free parameters are m_ϕ and ξ. The plots give the couplings in the m_ϕ, ξ parameter space.

  Note the hourglass shape that defines the theoretically allowed region.

- **The most important points**

  If $g^2_{fVh} < 1$ is observed then $m_\phi > m_h$, and vice versa, except for small region near $\xi = 0$.

  In cases where $g_{fV\phi}$ is small, prior indirect knowledge of, or constraints on, m_ϕ could be crucial.

  At large $|\xi|$, if $m_\phi > m_h$ the $ZZ\phi$ couplings can become sort of SM strength, implying SM type discovery modes could become relevant.

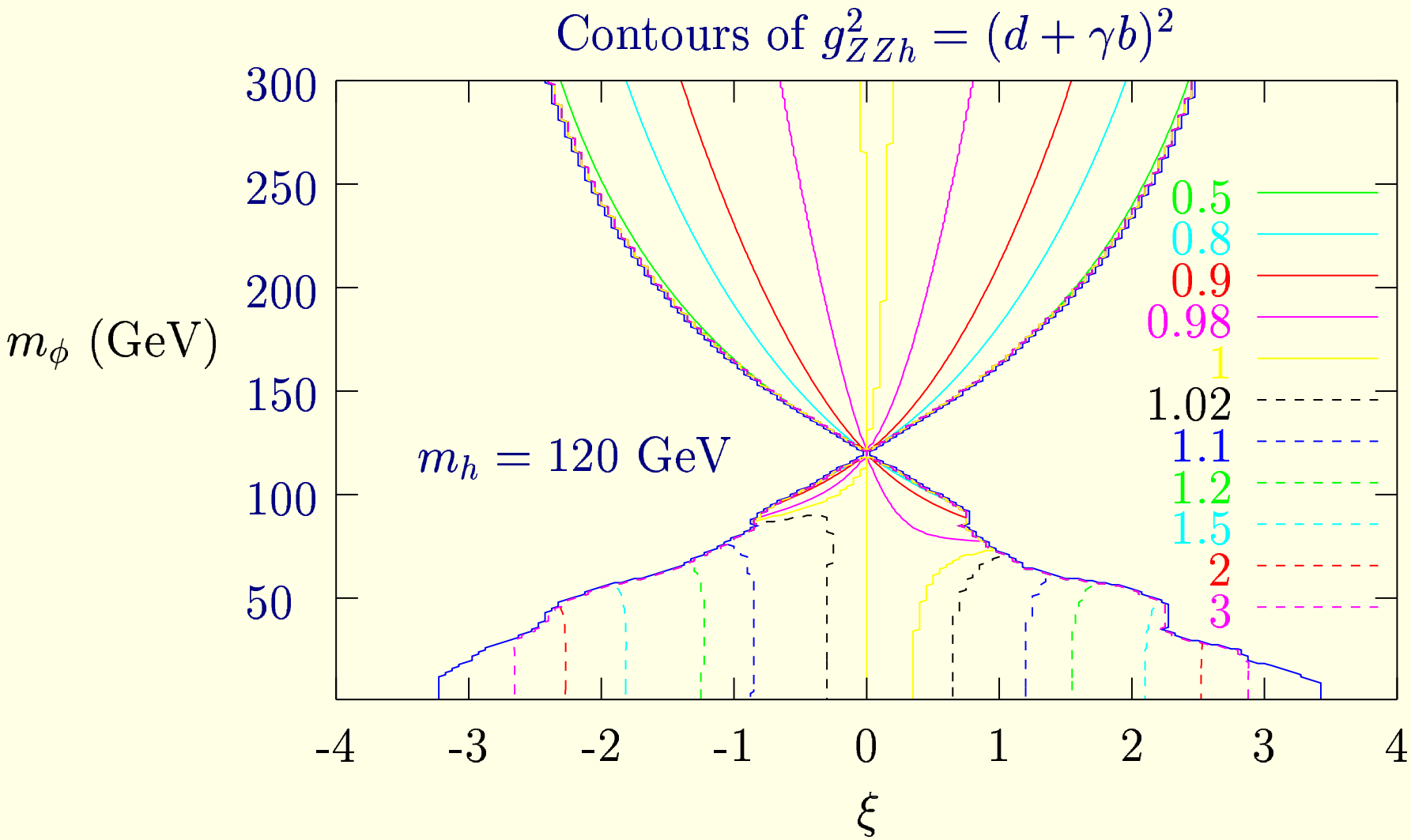

Figure 1: *Contours of* g^2_{fVh} *(relative to SM) for* $\Lambda_\phi = 5$ TeV, $m_h = 120$ GeV.

- **Observe suppression if** $m_\phi > m_h$ **and vice versa.**

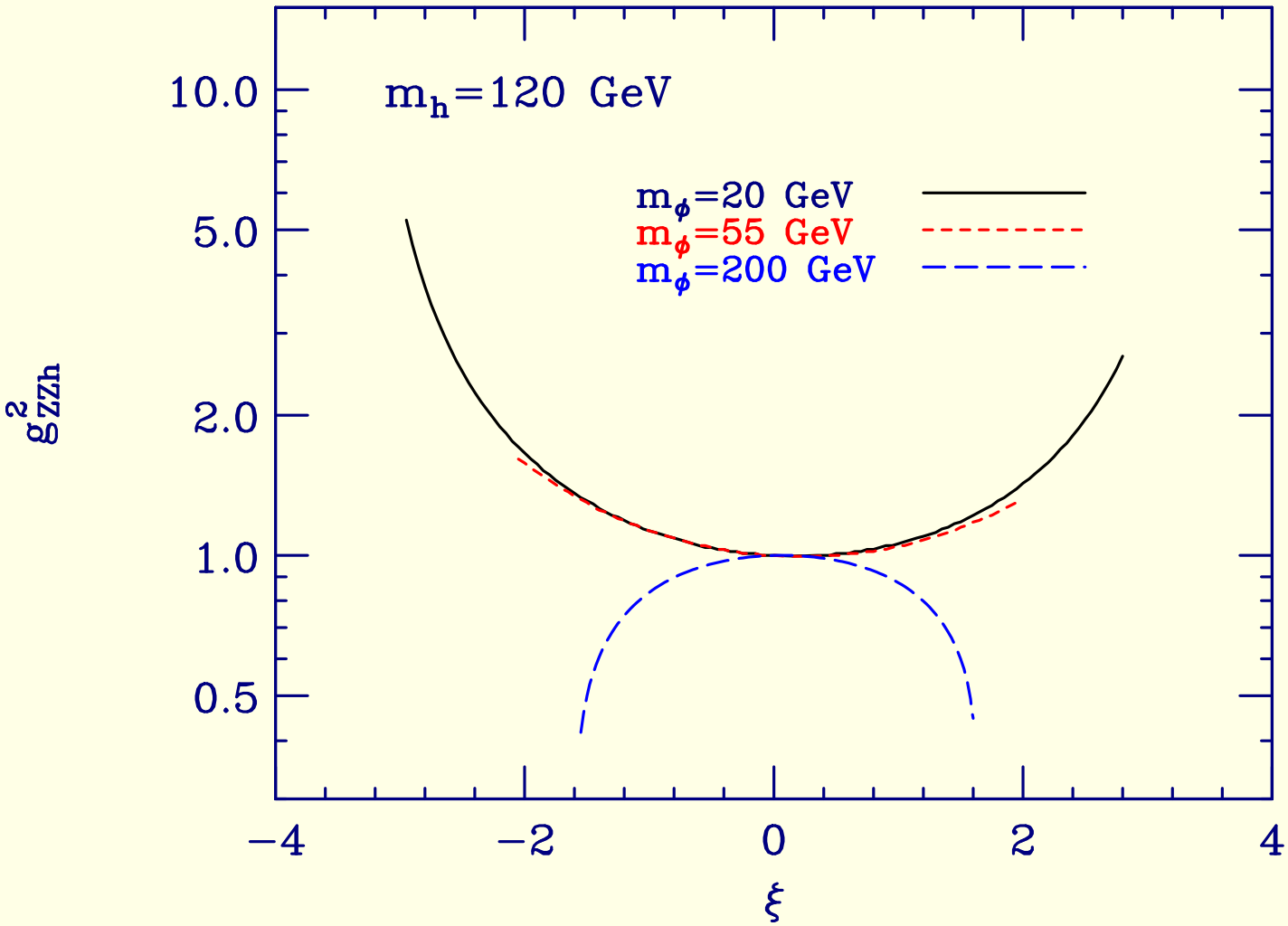

Figure 2: $g^2_{ZZh}/g^2_{ZZh_{\rm SM}} = g^2_{f\bar{f}h}/g^2_{f\bar{f}h_{\rm SM}}$ *as a function of* ξ *for several* m_ϕ *values.*

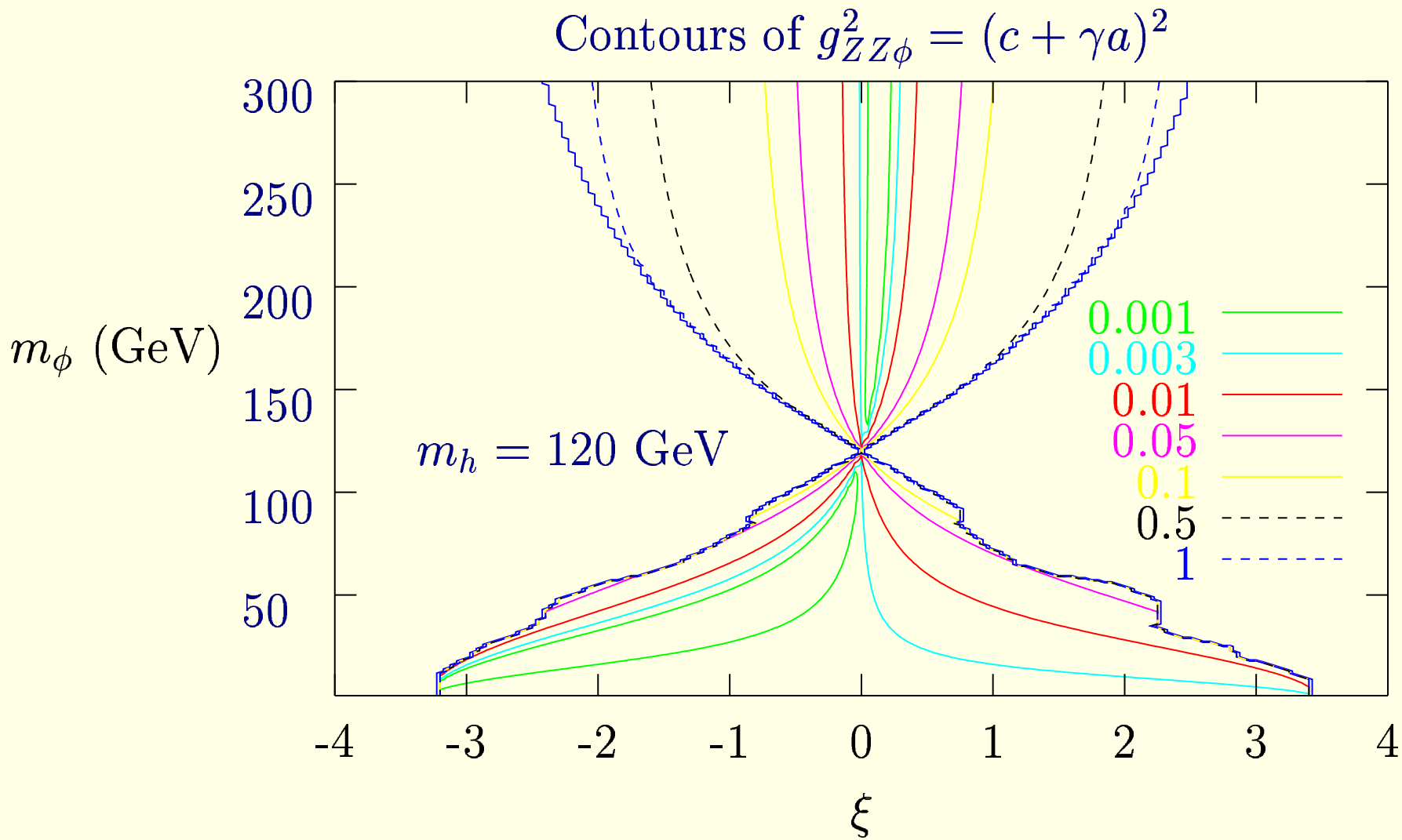

Figure 3: *Contours of* $g^2_{fV\phi}$ *for* $\Lambda_\phi = 5$ TeV, $m_h = 120$ GeV

- **Substantial** $g^2_{fV\phi}$ **is possible if** $m_\phi > m_h$ **and** ξ **is not too small.**

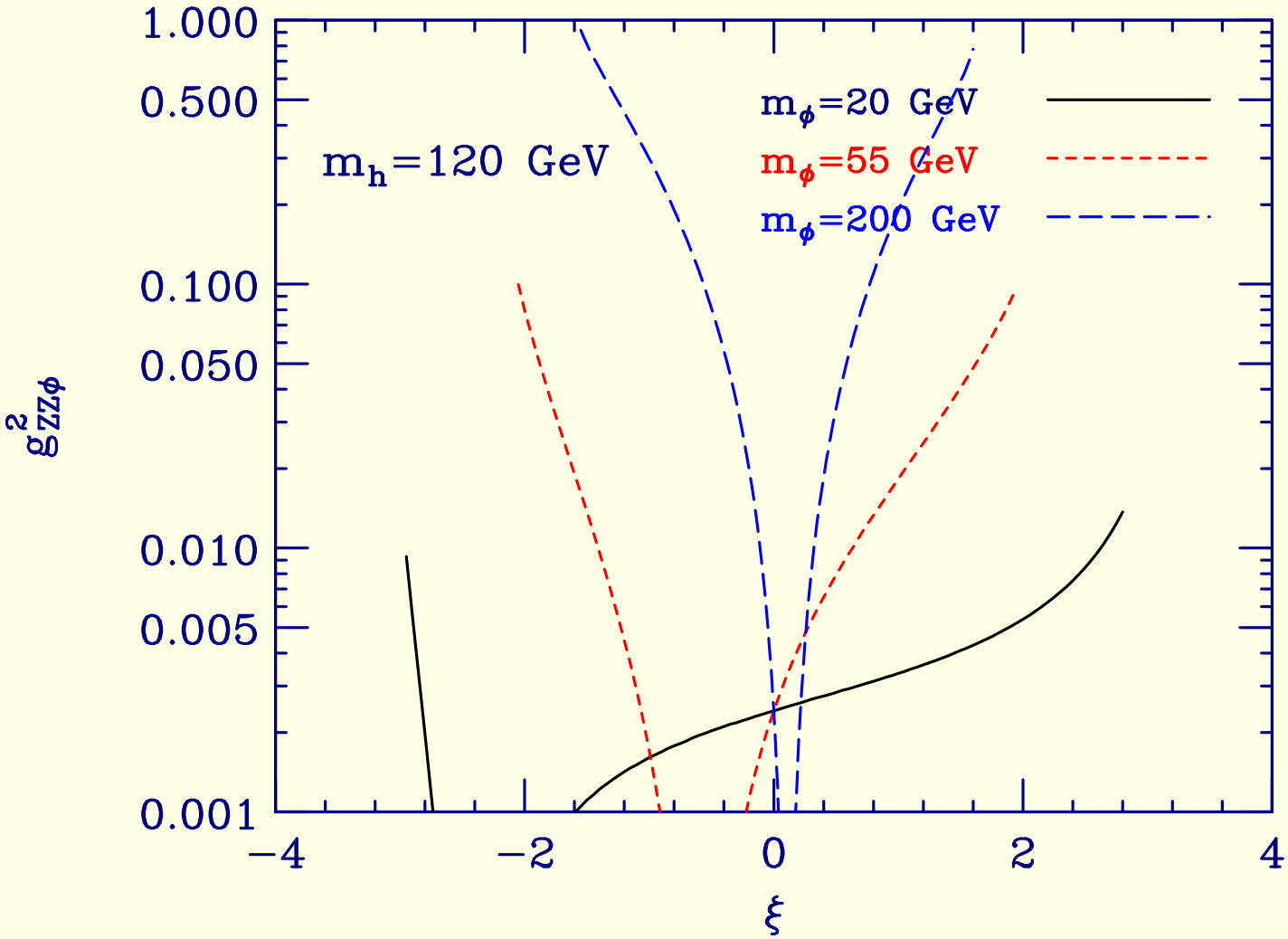

Figure 4: $g^2_{ZZ\phi}/g^2_{ZZh_{\rm SM}} = g^2_{f\bar{f}\phi}/g^2_{f\bar{f}h_{\rm SM}}$ *as a function of* ξ *for several* m_ϕ *values.*

Branching Ratios

Some important points are:

- h **branching ratios are quite SM-like (even if partial widths are different) except that** $h \to gg$ **can be bigger than normal, especially when** g^2_{fVh} **is suppressed.**

- **For** $m_\phi < 2m_W$, $\phi \to gg$ **is very possibly the dominant mode in the substantial regions near zeroes of** $g^2_{fV\phi}$.

  For $m_\phi > 2m_W$, ϕ **branching ratios are sort of SM-like (except at** $\xi \simeq 0$**) but total and partial widths are rescaled.**

LHC Capabilities

At the LHC, we (Battaglia, Dominici, de Curtis, de Roeck, JFG) focused on the case of a relatively light Higgs boson, $m_h = 120\ \mathrm{GeV}$ for example.

- The precision EW studies suggest that some of the larger $|\xi|$ range is excluded, but we studied the whole range just in case.

- We rescaled the statistical significances predicted for the SM Higgs boson at the LHC using the h and ϕ couplings predicted relative to the h_{SM}.

  A modified version of HDECAY was employed.

- The most important modes are $gg \to h \to \gamma\gamma$ and $gg \to \phi \to ZZ^{(*)} \to 4\ell$.

  Also useful are $t\bar{t}h$ with $h \to b\bar{b}$ and $h \to ZZ^* \to 4\ell$.

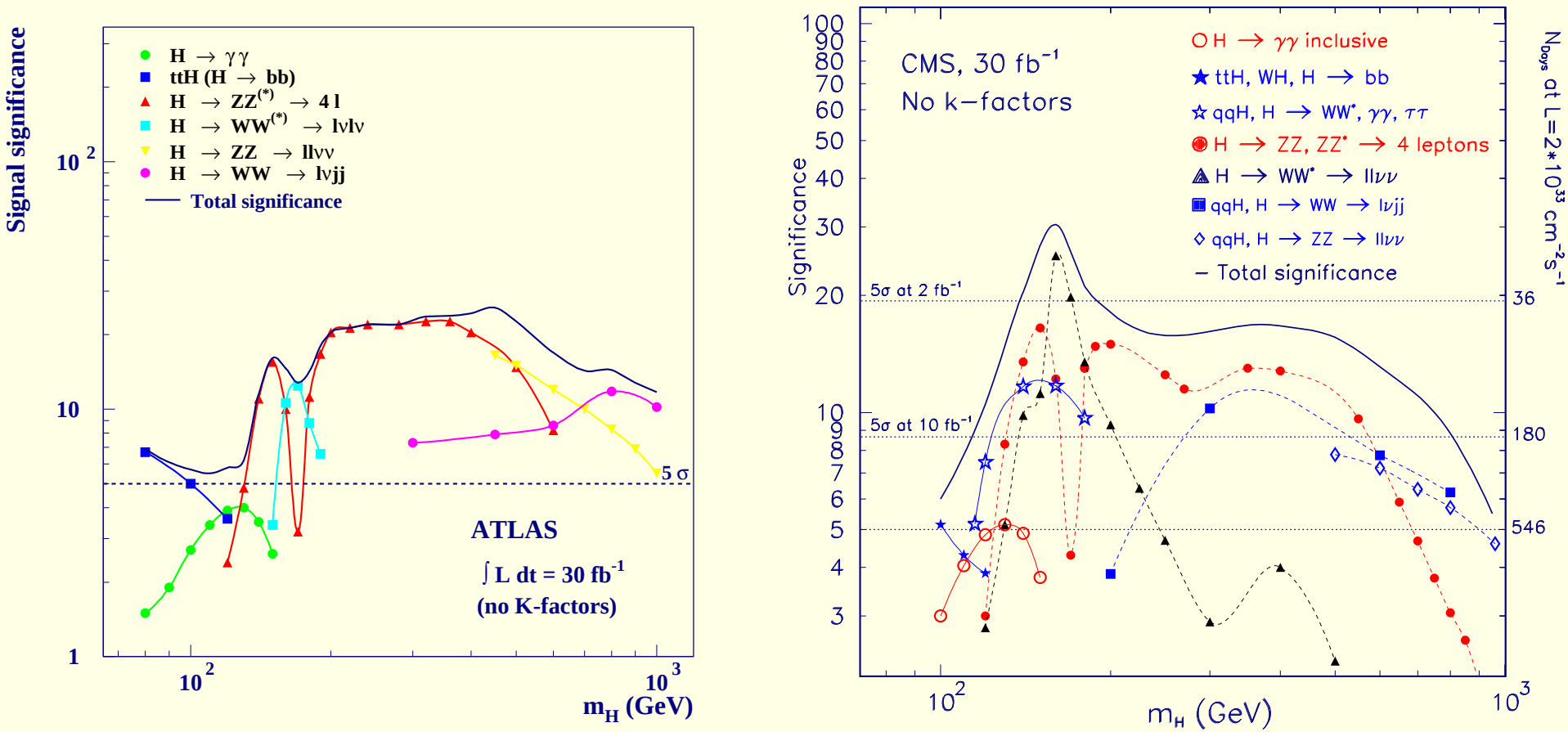

Figure 5: *SM Higgs search capabilities at the LHC for ATLAS and CMS.*

- **An example of the type of effect that will be observed is that the $h \to \gamma\gamma$ mode becomes unobservable if $|\xi|$ is large and $m_\phi > m_h$ (which together imply suppressed hWW coupling and hence suppressed W-loop**

contribution to the $\gamma\gamma h$ couplings).

One interesting graph is below. Note how we lose the $h \to \gamma\gamma$ mode if $m_\phi > m_h$, especially if $\xi < 0$. If $m_\phi < m_h$, $h \to \gamma\gamma$ will be strong if $\xi < 0$, but can be considerably weakened if $\xi > 0$.

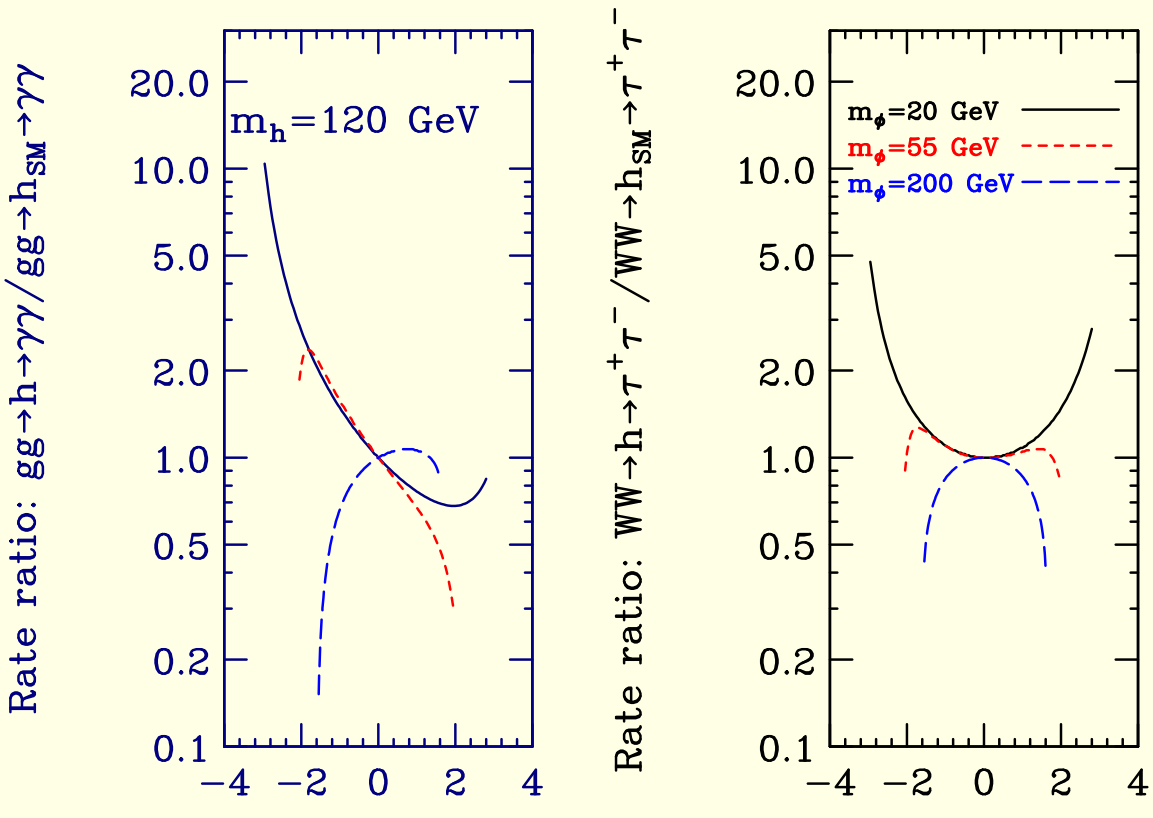

Figure 6: $gg \xrightarrow{\xi} h \to \gamma\gamma/gg \xrightarrow{\xi} h_{\rm SM} \to \gamma\gamma$ *and* $WW \to h \to \tau^+\tau^-/WW \to h_{\rm SM} \to \tau^+\tau^-$ *(same as for* $gg \to t\bar{t}h \to t\bar{t}b\bar{b}$*) for* $m_{h_{\rm SM}} = m_h$*;* $\Lambda_\phi = 5$ TeV.

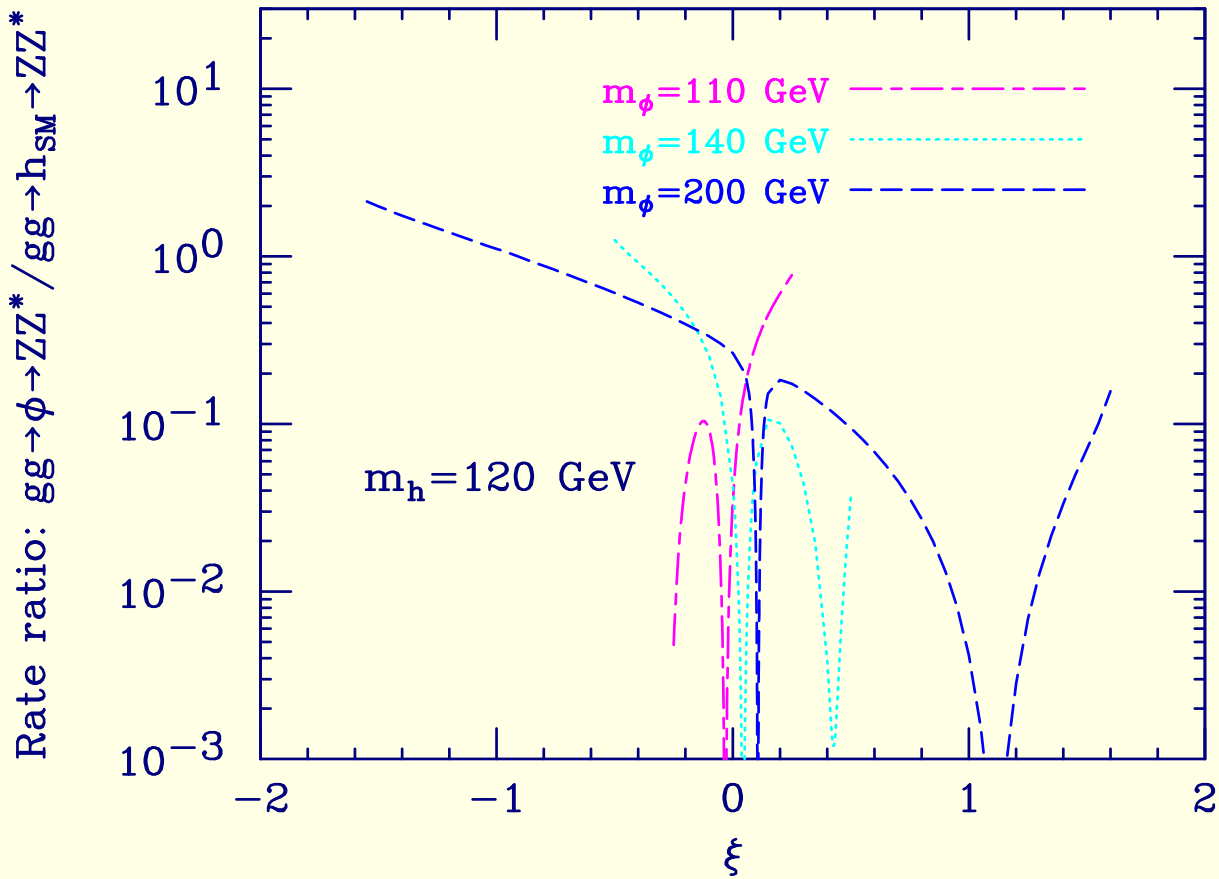

Figure 7: *The ratio of the rate for* $gg \to \phi \to ZZ$ *to the corresponding rate for a SM Higgs boson with mass* m_ϕ *assuming* $m_h = 120$ GeV *and* $\Lambda_\phi = 5$ TeV *as a function of* ξ *for* $m_\phi = 110$, 140 *and* 200 GeV. *Recall that the* ξ *range is increasingly restricted as* m_ϕ *becomes more degenerate with* m_h. *Note: for* $m_\phi > m_h$ *the mode approaches SM strength if* $\xi < 0$ *and is nearing SM strength if* $\xi > 0$ *and near maximal.*

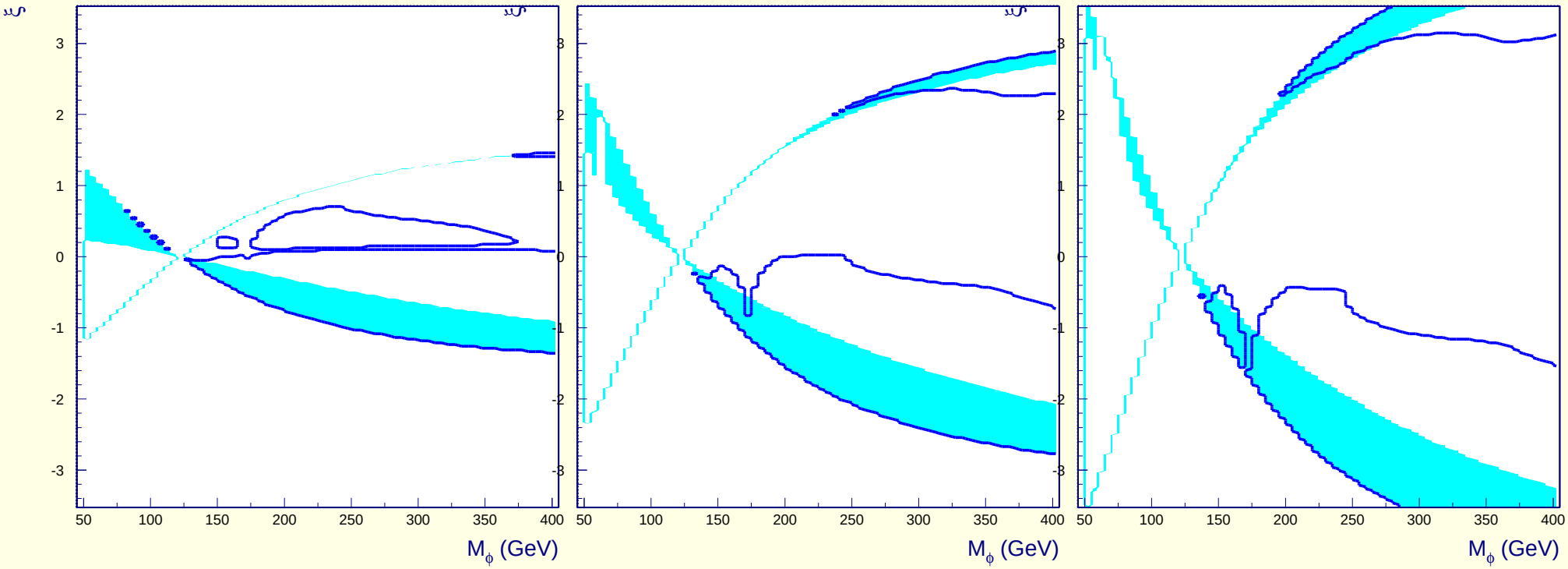

Figure 8: $L = 30\mathrm{fb}^{-1}$ *illustration of mode complementarity at the LHC for* $m_h = 120$ GeV. *The cyan regions show where the* $gg \to h \to \gamma\gamma$ *mode (or not very important at this* m_h *value,* $gg \to h \to 4\ell$ *mode) yields a* $> 5\sigma$ *signal. The regions between dark blue curves define the regions where* $gg \to \phi \to 4\ell$ *is* $> 5\sigma$. *The graphs are for* $\Lambda_\phi = 2.5$ TeV *(left)* $\Lambda_\phi = 5$ TeV *(center) and* $\Lambda_\phi = 7.5$ TeV *(right).*

The LHC can find either the h or ϕ except for the $m_\phi < m_h$, $\xi > 0$ and large, region.

But, some portion of this difficult region is disfavored by the precision electroweak data — e.g. $|\xi| \lesssim 1.5$ is preferred in the $\Lambda_\phi = 5$ TeV case.

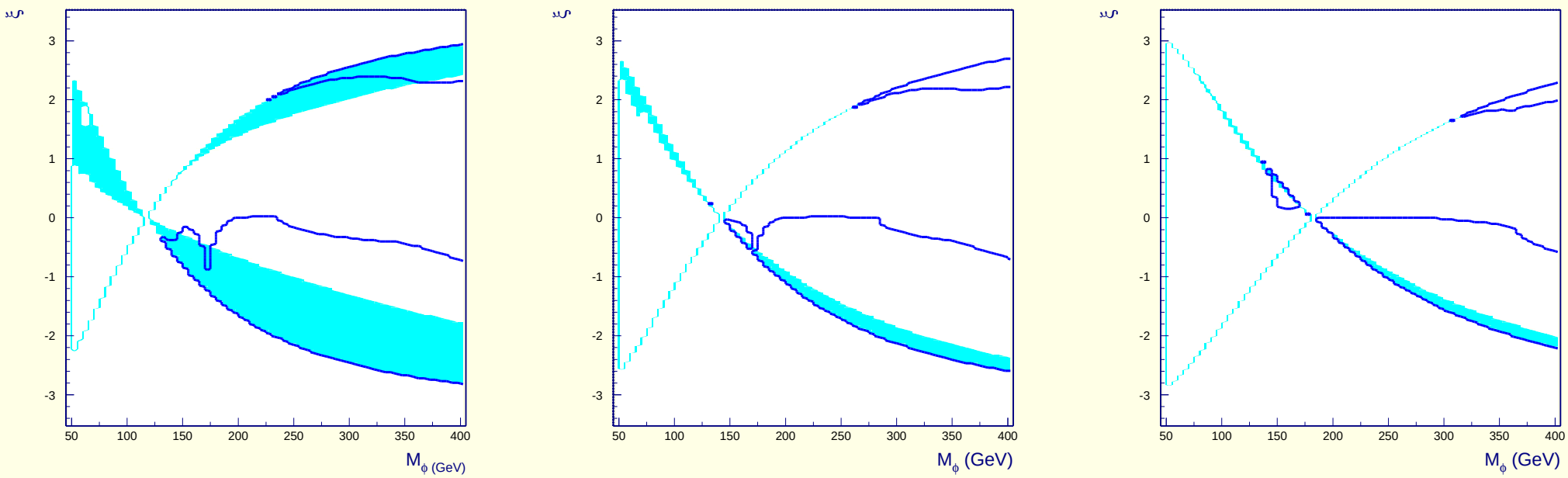

Figure 9: *As in previous figure. The graphs are for $\Lambda_\phi = 5$ TeV and $m_h = 115$ GeV (left) $m_h = 140$ GeV (center) and $m_h = 180$ GeV (right).*

Above, we see that the region where neither the h nor the ϕ can be

detected grows (decreases) as m_h decreases (increases). It diminishes as m_h increases since the $gg \to h \to 4\ell$ increases in strength at higher m_h.

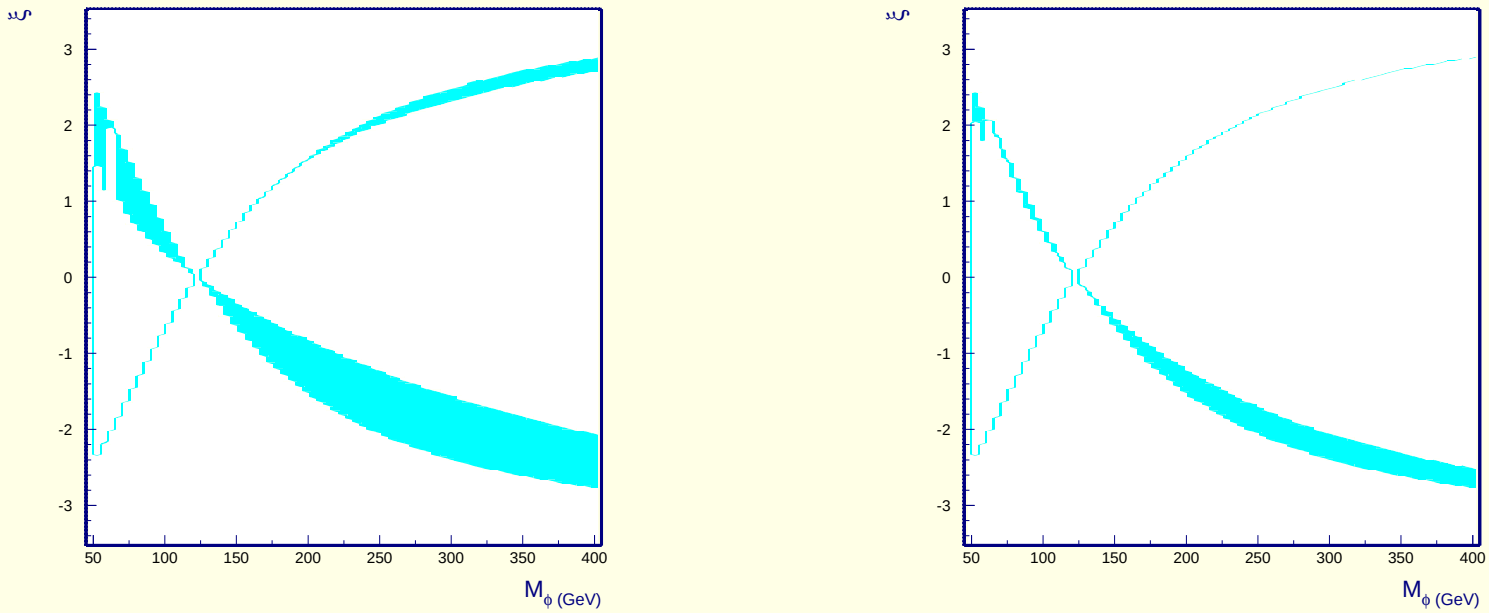

Figure 10: *The cyan regions are those where h discovery is not possible for $\Lambda_\phi = 5$ TeV and $m_h = 120$ GeV case assuming LHC $L = 30\mathrm{fb}^{-1}$ (left) or $L = 100\mathrm{fb}^{-1}$ (right).*

The regions where the h is not observable are reduced by considering either a larger data set or qqh Higgs production, in association with forward jets. An integrated luminosity of 100 fb^{-1} would remove the regions at large positive ξ in the $\Lambda_\phi = 5$ and 7.5 TeV plots of Fig. 8. Similarly,

including the qqh, $h \to WW^* \to \ell\ell\nu\bar{\nu}$ channel in the list of the discovery modes removes the same two regions and reduces the large region of h non-observability at negative ξ values.

- Figures 8 and 9 also exhibit regions of (m_h, ξ) parameter space in which *both* the h and ϕ mass eigenstates will be detectable.

  In these regions, the LHC will observe two scalar bosons somewhat separated in mass, with the lighter (heavier) having a non-SM-like rate for the gg-induced $\gamma\gamma$ (Z^0Z^0) final state.

  Additional information will be required to ascertain whether these two Higgs bosons derive from a multi-doublet or other type of extended Higgs sector or from the present type of model with Higgs-radion mixing.

- **What about an LC?**

  An e^+e^- LC should guarantee observation of both the h and the ϕ in the region of low m_ϕ, large $\xi > 0$ within which detection of either at the LHC might be difficult. This is because the $ZZ\phi$ coupling-squared is $\gtrsim 0.01$ relative to the SM for most of this region.

  But, what if there is no LC?

CLIC $\gamma\gamma$ Collider Capabilities

- **Let's remind ourselves about the results for the SM Higgs boson obtained in the CLIC study of hep-ex/0111056.**

  There, a SM Higgs boson with $m_{h_{\rm SM}} = 115$ GeV was examined.

  After the cuts, one obtains about $S = 3280$ and $B = 1660$ in the $\gamma\gamma \to h_{\rm SM} \to b\bar{b}$ channel, corresponding to $S/\sqrt{B} \sim 80$!!!

  We will assume that these numbers do not change significantly for a Higgs mass of 120 GeV.

- **After mixing, the S rate for the h will be rescaled relative to that for the $h_{\rm SM}$. Of course, B will not change.**

  The rescaling is shown in the figure.

- **The S for the ϕ can also be obtained by rescaling if $m_\phi \sim 115$ GeV.**

  For $m_\phi < 120$ GeV, the $\phi \to b\bar{b}$ channel will continue to be the most relevant for ϕ discovery, but studies have not yet been performed to obtain the S and B rates for low masses.

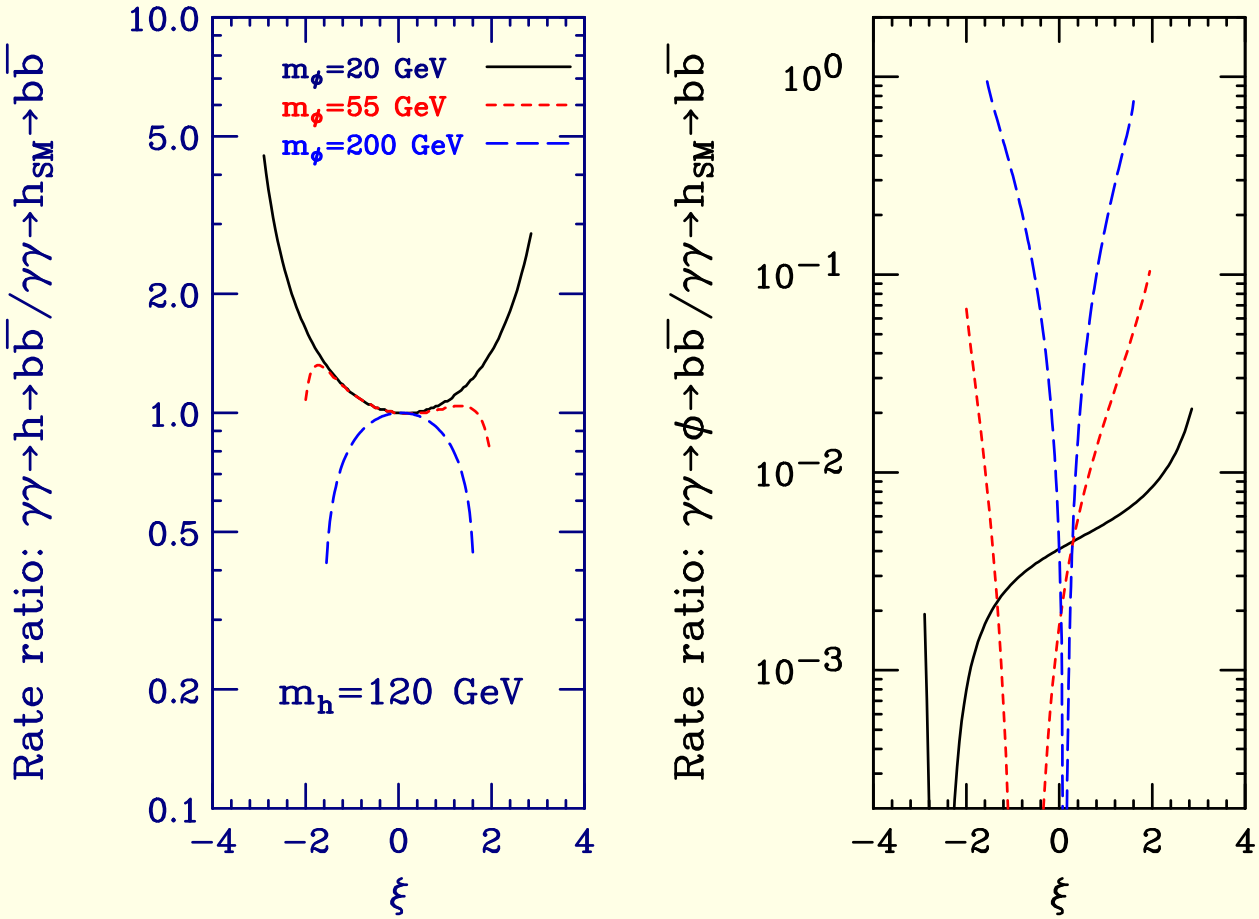

Figure 11: The rates for $\gamma\gamma \to h \to b\bar{b}$ and $\gamma\gamma \to \phi \to b\bar{b}$ relative to the corresponding rate for a SM Higgs boson of the same mass. Results are shown for $m_h = 120$ GeV and $\Lambda_\phi = 5$ TeV as functions of ξ for $m_\phi = 20$, 55 and 200 GeV.

Observe that for $m_\phi < m_h$ we have either little change or enhancement, whereas significant suppression of the $gg \to h \to \gamma\gamma$ rate was possible in this case for positive ξ.

Also note that for $m_\phi > m_h$ and large $\xi < 0$ (where the LHC could not see the h) there is much less suppression of $\gamma\gamma \to h \to b\bar{b}$ than for $gg \to h \to \gamma\gamma$ — at most a factor of 2 vs a factor of 8 (at $m_\phi = 200\ \mathrm{GeV}$).

This is no problem since $S/\sqrt{B} \sim \frac{1}{2}80 \sim 40$ is still a very strong signal.

- In fact, we can afford a reduction by a factor of 16 before we hit the 5σ level!

- Thus, *the $\gamma\gamma$ collider will allow h discovery (for $m_h = 120$) throughout the entire hourglass*, which is something the LHC cannot do.

- Using the factor of 16 mentioned above, the ϕ with $m_\phi < 120\ \mathrm{GeV}$ is very likely to elude discovery at the $\gamma\gamma$ collider. (Recall that it also eludes discovery at the LHC for this region.)

  The only exceptions to this statement occur at the very largest $|\xi|$ values for $m_\phi \geq 55\ \mathrm{GeV}$ where $S_\phi > S_{h_{\rm SM}}/16$.

- Of course, we need to have signal and background results after cuts for

these lower masses to know if the factor of 16 is actually the correct factor to use.

To get the best signal to background ratio we would want to lower the machine energy (relatively easy for CLIC case) and readjust cuts and so forth.

This study should be done.

- **For the $m_\phi > m_h$ region, we will need results for the WW and ZZ modes that are being worked on.**

Conclusions

- **The γC is more than competitive with the LHC for h discovery.**

  The γC can see the h where the LHC can't, although the "bad" LHC regions are not very big for full L.

- **Of course, there is a big part of the hourglass where the h will be seen at both colliders.**

  This is most of the hourglass when L at the LHC is $> 100\mathrm{fb}^{-1}$.

  This will certainly increase our knowledge about the h since the two rates measure different things.

  The ratio of the rates gives us $\frac{\Gamma(h\to gg)}{\Gamma(h\to b\bar{b})}$, in terms of which we may compute

$$R_{hgg} \equiv \left[\frac{\Gamma(h\to gg)}{\Gamma(h\to b\bar{b})}\right]\left[\frac{\Gamma(h\to gg)}{\Gamma(h\to b\bar{b})}\right]_{SM}^{-1} . \tag{11}$$

  This is a very!!!! interesting number since it directly probes for the presence of the anomalous ggh coupling.

In particular, $R_{hgg} = 1$ if the only contributions to $\Gamma(h \to gg)$ come from quark loops and all quark couplings scale in the same way.

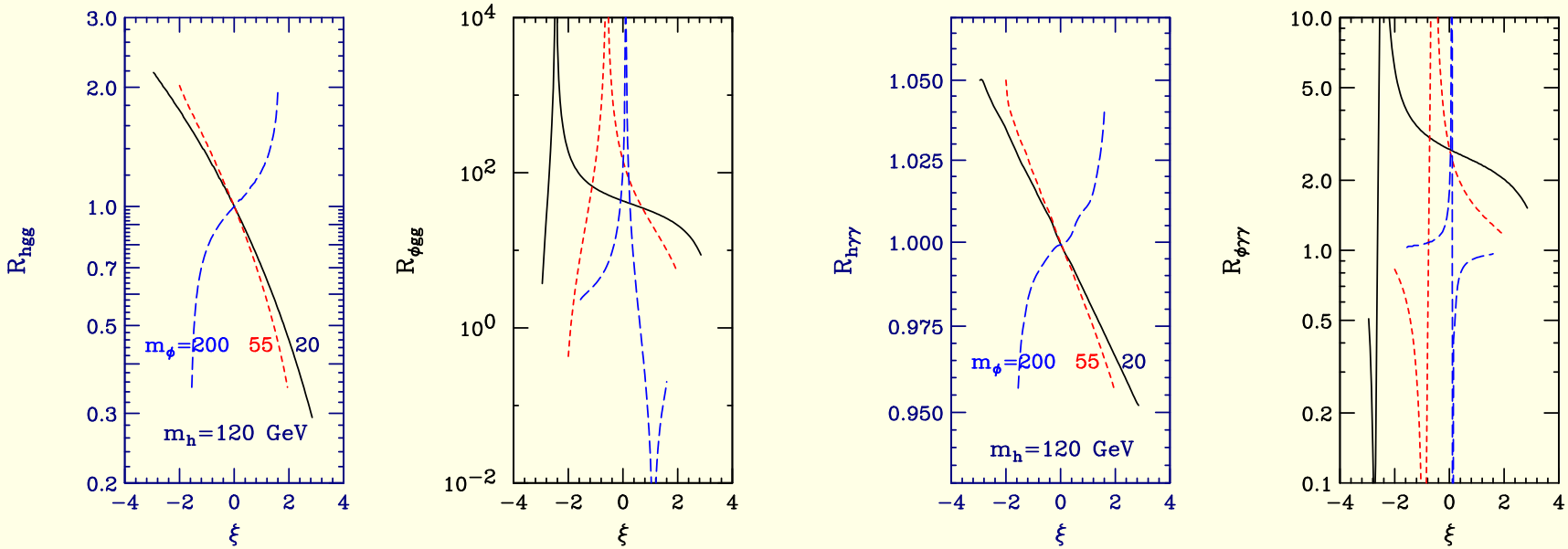

Figure 12: *In the left two plots, we give the ratios R_{hgg} and $R_{\phi gg}$ of the hgg and ϕgg couplings-squared including the anomalous contribution to the corresponding values expected in its absence. Results for the the analogous ratios $R_{h\gamma\gamma}$ and $R_{\phi\gamma\gamma}$ are presented in the two plots on the right. Results are shown for $m_h = 120$ GeV and $\Lambda_\phi = 5$ TeV as functions of ξ for $m_\phi = 20$, 55 and 200 GeV. (The same type of line is used for a given m_ϕ in the right-hand figure as is used in the left-hand figure.)*

We can estimate the accuracy with which R_{hgg} can be measured as follows. Assuming the maximal reduction of 1/2 for the S rescaling at the $\gamma\gamma$ CLIC collider, we find that $\Gamma(h \to \gamma\gamma)\Gamma(h \to b\bar{b})/\Gamma^h_{tot}$ can be measured with an accuracy of about $\sqrt{S+B}/S \sim \sqrt{3200}/1600 \sim 0.035$. The dominant error will then be from the LHC which will typically measure $\Gamma(h \to gg)\Gamma(h \to \gamma\gamma)/\Gamma^h_{tot}$ with an accuracy of between 0.1 and 0.2 (depending on parameter choices and available L). From Fig. 12, we see that 0.2 fractional accuracy will reveal deviations of R_{hgg} from 1 for all but the smallest ξ values.

- The ability to measure R_{hgg} may be the strongest reason in the Higgs context for having the γC as well as the LHC.

  Almost all non-SM Higgs theories predict $R_{hgg} \neq 1$ for one reason another, unless one is in the decoupling limit.

- Depending on L at the LHC, there is a somewhat smaller part of the hourglass (large $|\xi|$ with $m_\phi > m_h$) where *only* the ϕ will be seen at the LHC and the h will only be seen at the γC.

  (We don't know for sure about the ϕ at the γC until WW, ZZ final states are studied, but I am not all that optimistic.)

This is a nice example of complementarity between the two machines. By having both machines we maximize the chance of seeing both the h and ϕ.

- **Thus, there is a strong case for the γC in the RS model context!, especially if a Higgs boson is seen at the LHC that has non-SM-like rates, ...**